Supplementary Information (SI) for Journal of Materials Chemistry C.
This journal is © The Royal Society of Chemistry 2025

Supporting information

Integration of a symmetric D-A-D chromophore with biocompatible silk fibroin for ultrafast measurement and flexible solid-state lasing

Ja-Hon Lin,[*a] Hsin-Yi Wei,[a] Wei-Chen Tsai,[a] Yu-Cheng Hou,[a] Yun-Yi Kao,[b] Tzu-Chau Lin,[*b] Ayano Abe,[c] and Chihaya Adachi,[*c]

E-mail: jhlin@ntut.edu.tw; tclin@ncu.edu.tw; adachi@cstf.kyushu-u.ac.jp

[a.] Department of Electro-Optical Engineering, Advanced Nanophotonics Technology Laboratory, National Taipei University of Technology, Taipei 10608, Taiwan.
E-mail: jhlin@ntut.edu.tw (J.-H. Lin)

[b.] Photonic Materials Research Laboratory, Department of Chemistry, National Central University, Taoyuan City 32001, Taiwan.
E-mail: tclin@ncu.edu.tw

[c.] Center for Organic Photonics and Electronics Research (OPERA) and International Institute for Carbon Neutral Energy Research (WPI-I2CNER), Kyushu University, Fukuoka 819-0395, Japan.
E-mail: adachi@cstf.kyushu-u.ac.jp

◆ **Numbering of C and H for the synthons (Compounds 3-7)**

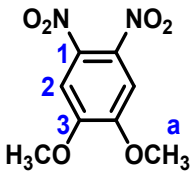

3

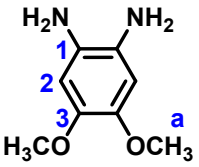

4

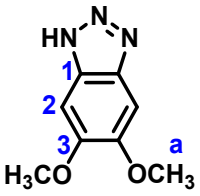

5

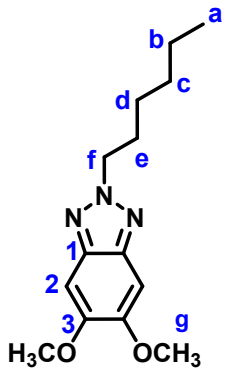

6a

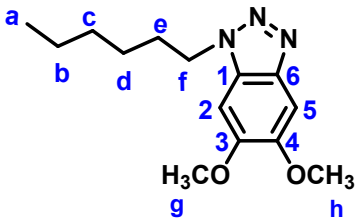

6b

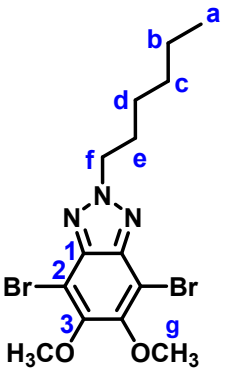

7

◆ **Numbering of C and H for the final chromophore (Compound 1)**

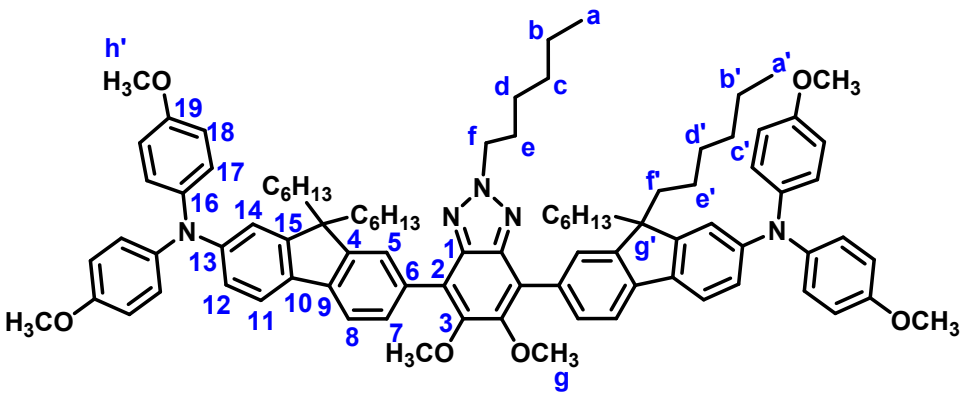

1

1,2-Dimethoxy-4,5-dinitrobenzene (3)

Compound **2** (5 g, 36.21 mmol) was added into nitric acid (47 mL) at 0°C and the resulting solution was stirred at 80 °C for 2 h. After cooled down to r.t., the reaction mixture was poured into crushed ice, stirred, and filtered. The collected crude product was recrystallized from ethanol and the purified product was obtained as yellow powder (6.9 g; yield = 85 %). ^{1}H NMR (300 MHz, $CDCl_3$): δ 7.33 (s, 2H, H_2), 4.00 (s, 6H, H_a); ^{13}C NMR (75 MHz, $CDCl_3$): δ 151.07 (C_3), 136.42 (C_1), 106.77 (C_2), 56.84 (C_a).

4,5-Dimethoxybenzene-1,2-diamine (4)

A mixture of compound **3** (3 g, 13.1 mmol) and $SnCl_2{\cdot}2H_2O$ (29.67 g, 131 mmol) in ethanol (75 mL) and HCl (60 mL) was refluxed overnight. After cooled down to r.t., the solvent was removed by rotary evaporator. To the mixed residue was added 5 M NaOH (75 mL) and adjust the pH value of the resulting solution to pH = 10. The above-mentioned solution was extracted by dichloromethane (100 mL × 3). The organic layer was collected, dried over $MgSO_{4(s),}$ and filtered. After removal of the solvent, the pure product was obtained as white powder (2.04 g; yield = 93 %). ^{1}H NMR (500 MHz, $CDCl_3$) δ: 6.39 (s, 2H, H_2), 3.08 (s, 6H, H_a), 3.23 (s, 4H, H_b); ^{13}C NMR (125 MHz, $CDCl_3$): δ 142.97 (C_3), 127.64 (C_1), 103.77 (C_2), 56.61(C_a).

5,6-Dimethoxy-1*H*-benzo[*d*][1,2,3]triazole (5)

To a mixture of compound **4** (2 g, 10.98 mmol) in acetic acid (20 mL) and H_2O (5 mL) was added aqueous $NaNO_2$ (1.96 g, 28.47 mmol/ 5 mL H_2O) and the resulting solution was stirred at r.t. for overnight. After the reaction is completed, a saturated $NaHCO_{3(aq)}$ was added to neutralize the reaction mixture and this mixed solution was extracted by ethyl acetate (50 mL × 3) and the organic layer was collected and dried over $MgSO_{4(s).}$ The solvent was removed by rotary evaporator and the pure product was obtained as

orange solid (1.32 g; yield = 63 %). ^{1}H NMR (500 MHz, $CDCl_3$): δ 7.21 (s, 2H, H_2), 3.94 (s, 6H, H_a), 9.87 (s, 1H, H_b); ^{13}C NMR (125 MHz, $CDCl_3$): δ 150.60 (C_3), 134.01 (C_1), 94.35 (C_2), 56.22(C_a).

5,6-Dimethoxy-2-hexyl-2*H*-benzo[*d*][1,2,3]triazole (6a) &

5,6-Dimethoxy-1-hexyl-2*H*-benzo[*d*][1,2,3]triazole (6b)

A mixture composed of compound **5** (1.3 g, 17.22 mmol) and NaO^tBu (1.04 g, 10.8 mmol) in methanol (17 mL) was refluxed for 30 minutes before the addition of bromohexane (1.54 mL, 10.83 mmol). The resulting reaction mixture was then heated to reflux for overnight. After reaction was completed, 1 mL of pyridine was added into the reaction mixture and the whole system was refluxed for another 1 h. After cooled down to r.t., the solvent was removed from the reaction mixture by rotary evaporator and the residue was re-dissolved in ethyl acetate (50 mL), which is mixed with 1N $HCl_{(aq)}$ (5 mL) and stirred for 30 min. The above solution was extracted with ethyl acetate (50 mL × 3) and the organic layer was collected and dried over $MgSO_{4(s)}$. After filtration and removal of solvent from the filtrate, the residue was purified by column chromatography on silica gel using *n*-hexane: ethyl acetate (1:1) as eluent to afford two separable isomers:

Compound 6a: Yellow liquid (0.8 g; yield = 42 %). ^{1}H NMR (500 MHz, $CDCl_3$): δ 6.97 (s, 2H, H_2, H_5), 4.44 (t, *J*= 6.9 Hz, 2H, H_f), 3.82 (s, 6H, H_a), 1.91-1.96 (m, 2H; H_e), 1.13-1.19 (m, 6H; H_b, H_c, H_d), 0.75 (t, *J*= 6 Hz, 3H; H_a); ^{13}C NMR (125 MHz, $CDCl_3$): δ 150.63 (C_3), 139.27 (C_1), 94.99 (C_2), 55.52 (C_g), 55.44 (C_f), 30.75 (C_e), 29.55 (C_d), 25.76 (C_c), 21.94 (C_b), 13.46 (C_a).

Compound 6b: Orange liquid (0.76 g; yield = 40 %). ^{1}H NMR (500 MHz, $CDCl_3$) δ: 7.35 (s, 1H, H_5) 6.78 (s, 1H, H_2), 4.54 (t, *J*= 7 Hz, 2H; H_f), 3.98 (s, 6H; H_g, H_h), 1.96-1.99 (m, 2H, H_e), 1.27-1.34 (m, 6H; H_b, H_c, H_d), 0.86 (t, *J*= 6.5 Hz, 3H, H_a); ^{13}C NMR

(125 MHz, $CDCl_3$): δ 150.76 (C_4), 147.99 (C_3), 139.66 (C_6),127.53(C_1), 98.07 (C_5), 89.19 (C_2), 55.73 (C_h), 55.54 (C_g), 47.39(C_f), 30.56 (C_e), 28.93 (C_d), 25.72 (C_c), 21.80 (C_b), 13.30 (C_a).

4,7-Dibromo-5,6-dimethoxy-2-hexyl-2*H*-benzo[*d*][1,2,3]triazole (7)

To a mixture of compound **6a** (0.7 g, 2.60 mmol) in dichoromethane (37 mL) and acetic acid (18 mL) was added bromine (1 mL, 19.6 mmol) and the reaction mixture was stirred at r.t. for 40 h. After the reaction was completed, the reaction mixture was poured into a 300 mL water and quenched with saturated $NaHSO_{3(aq)}$. The resulting solution was extracted by dichloromethane (50 mL × 3). The organic layer was collected and dried over $MgSO_{4(s)}$. After filtration and removal of the solvent, the pure product was obtained as yellow liquid (1.1 g; yield = 93 %). ^{1}H NMR (500 MHz, $CDCl_3$): δ 4.71 (t, *J*= 7.5 Hz, 2H; H_f), 3.96 (s, 6H, H_a), 2.06-2.12 (m, 2H, H_e), 1.28-1.36 (m, 6H; H_b, H_c, H_d), 0.86 (t, *J*= 7 Hz, 3H; H_a); ^{13}C NMR (125 MHz, $CDCl_3$): δ 151.85 (C_3), 140.50 (C_1), 102.83 (C_2), 61.42 (C_g), 57.11 (C_f), 31.08 (C_e), 30.09 (C_d), 26.10 (C_c), 22.32 (C_b), 13.84 (C_a). HRMS (FAB): *m/z*: calcd for $C_{14}H_{20}Br_2N_3O_2$, 419.9944; found 419.9917 [(^{79}Br)(^{79}Br)M]$^+$, 421.9897 [(^{79}Br)(^{81}Br)-M]$^+$, 423.9878 [(^{81}Br)(^{81}Br)M]$^+$.

7,7'-(2-Hexyl-5,6-dimethoxy-2*H*-benzo[*d*][1,2,3]triazole-4,7-diyl)bis(9,9-dihexyl-*N*,*N*-bis-(4-methoxyphenyl)-9*H*-fluoren-2-amine) (1)

To a 250 mL round-bottom flask was charged compound **7** (0.7g, 1.6 mmol), compound **8** (2.42 g, 3.5 mmol), K_2CO_3 (1.8 g, 13.28 mmol), $Pd(PPh_3)_4$ (0.19 g, 0.166 mmol), H_2O (7 mL) and 1,4-dioxane (21 mL) and the resulting solution was refluxed for 24 h. After cooled down to r.t., the solution was filtered through a pad of Celite 545 and the filtrate was extracted with dichloromethane (50 mL × 3). The organic layer was collected and dried over $MgSO_{4(s)}$ and after filtration and removal of the solvent, the residue product

was purified by precipitation method in a binary solvent system composed of dichloromethane and methanol. The final product was obtained as bright yellow solid (1.67 g; yield = 73 %). ^{1}H NMR δ: 7.85 (d, *J*=7 Hz, 4H; H_8), 7.72 (d, *J*=8.5Hz, 2H; H_{11}), 7.54 (d, *J*=8 Hz, 2H; H_7), 7.09 (d, *J*=9 Hz, 8H; H_{18}), 7.03 (s, J_2=2 Hz, 2H; H_{14}), 6.91 (dd, J_1= 8.5 Hz, J_2= 2 Hz, 2H; H_{12}), 6.84 (d, *J*=8 Hz, 8H; H_{17}), 4.67 (t, *J*=7.5 Hz, 2H; H_f), 3.82 (s, 12H; $H_{h'}$), 3.72 (s, 6H; H_g), 2.05-2.08 (m, 2H; H_e), 1.82-1.97 (m, 8H; $H_{f'}$), 1.31-1.39 (m, 6H; H_b, H_c, H_d), 1.09-1.18 (m, 24H; $H_{c'}$, $H_{d'}$, $H_{e'}$), 0.87 (t, *J*=7 Hz, 3H, H_a), 0.81 (t, *J*= 5 Hz, 20H; $H_{a'}$, $H_{b'}$); ^{13}C NMR (125 MHz, $CDCl_3$): δ 155.44 (C_{19}), 152.51 (C_3), 150.47 (C_4), 150.01 (C_{15}), 148.13 (C_1), 141.59 (C_{16}), 141.24 (C_{10}), 140.69 (C_9), 134.52 (C_{13}), 131.24 (C_6), 128.92 (C_2), 125.85 (C_{18}), 125.06 (C_8), 122.44 (C_7), 120.71 (C_5), 120.15 (C_{11}), 118.48 (C_{14}), 116.56 (C_{12}), 61.08 (C_g) , 56.49 (C_f), 55.47 ($C_{h'}$), 54.97 ($C_{g'}$), 40.32 ($C_{f'}$), 31.60 ($C_{e'}$), 31.26 (C_e), 30.12 ($C_{d'}$), 29.79 (C_d) 26.28 (C_c), 23.92 ($C_{c'}$), 22.59 ($C_{b'}$), 22.48 (C_b), 14.00 ($C_{a'}$), 13.93 (C_a). HRMS (MALDI-TOF): *m/z*: calcd for $C_{92}H_{111}N_5O_6$: 1382.8562 $[M+1]^+$: found 1382.8119.

♦1H and 13C NMR spectra of the precursors and final compound

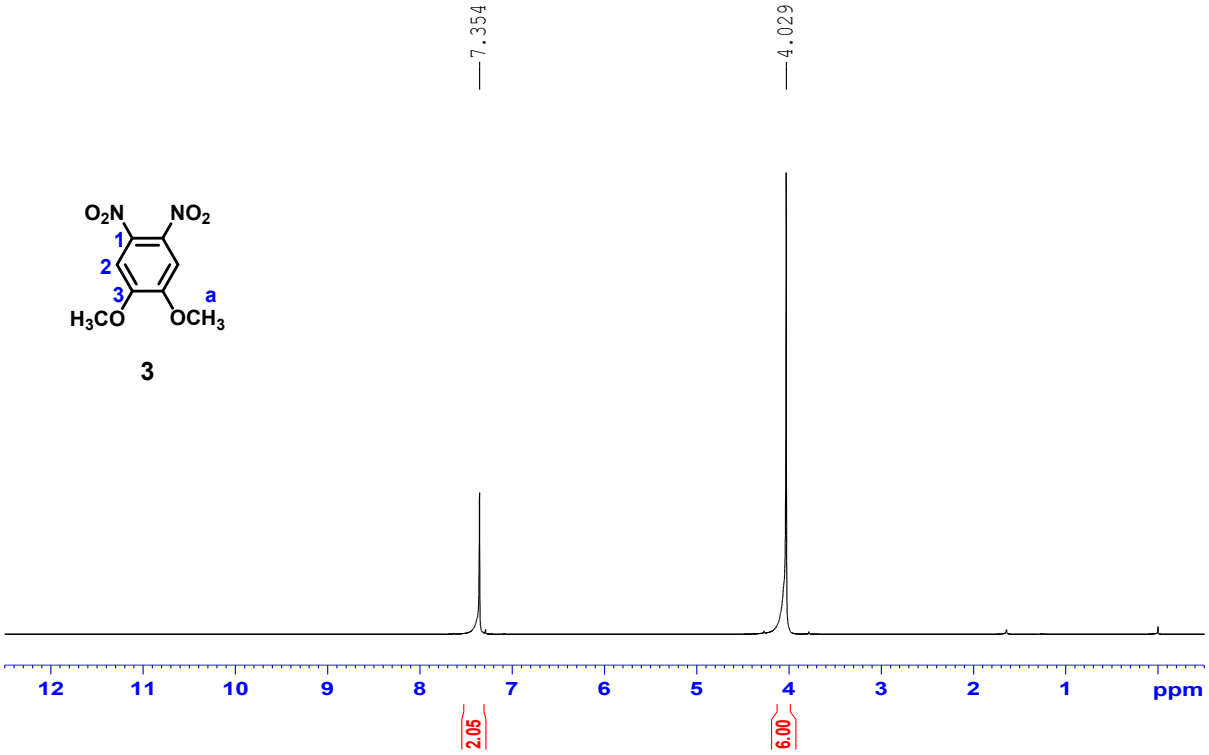

^{1}H NMR Spectrum of Compound 3 (Solvent: $CDCl_3$)

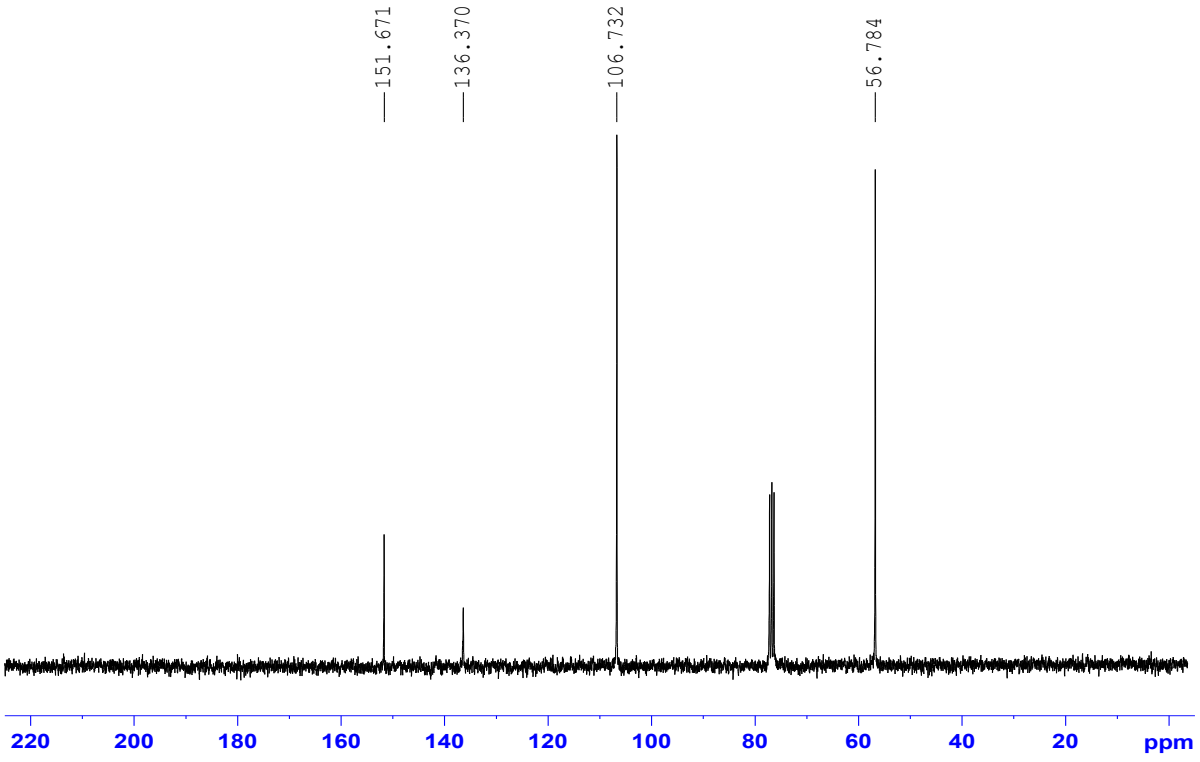

13C NMR Spectrum of Compound 3 (Solvent: CDCl3)

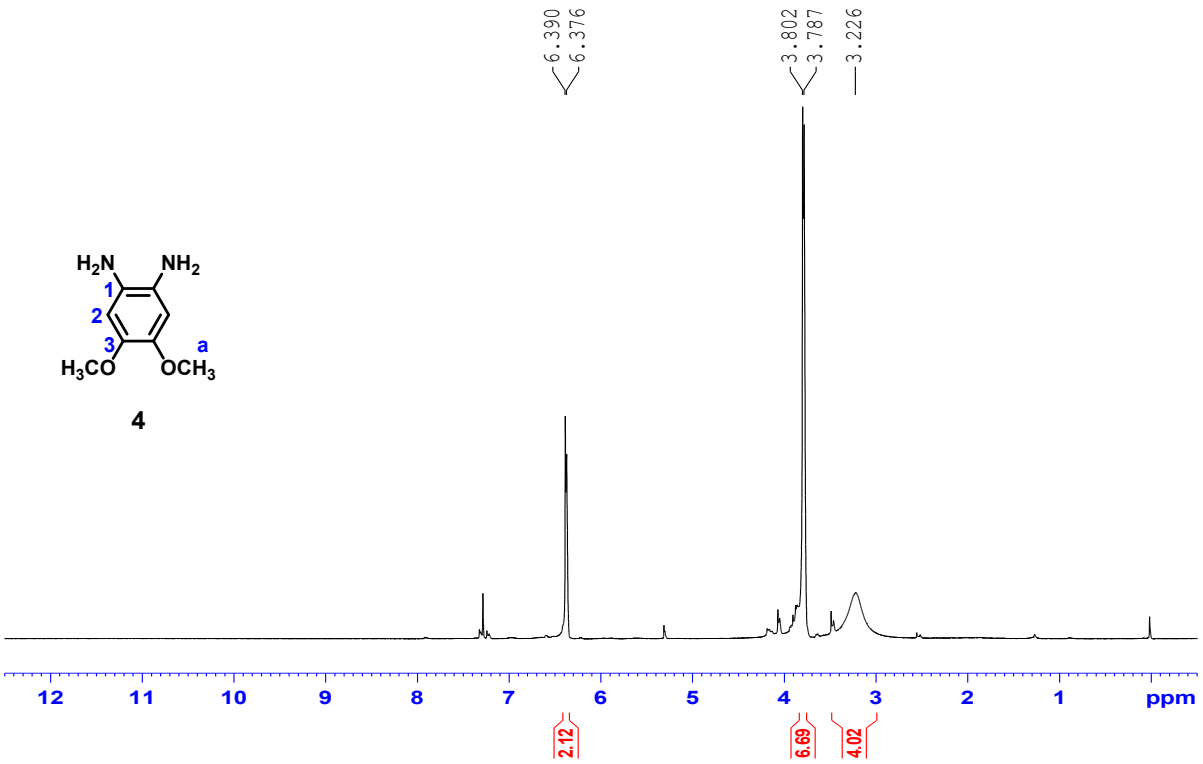

^{1}H NMR Spectrum of Compound 4 (Solvent: $CDCl_3$)

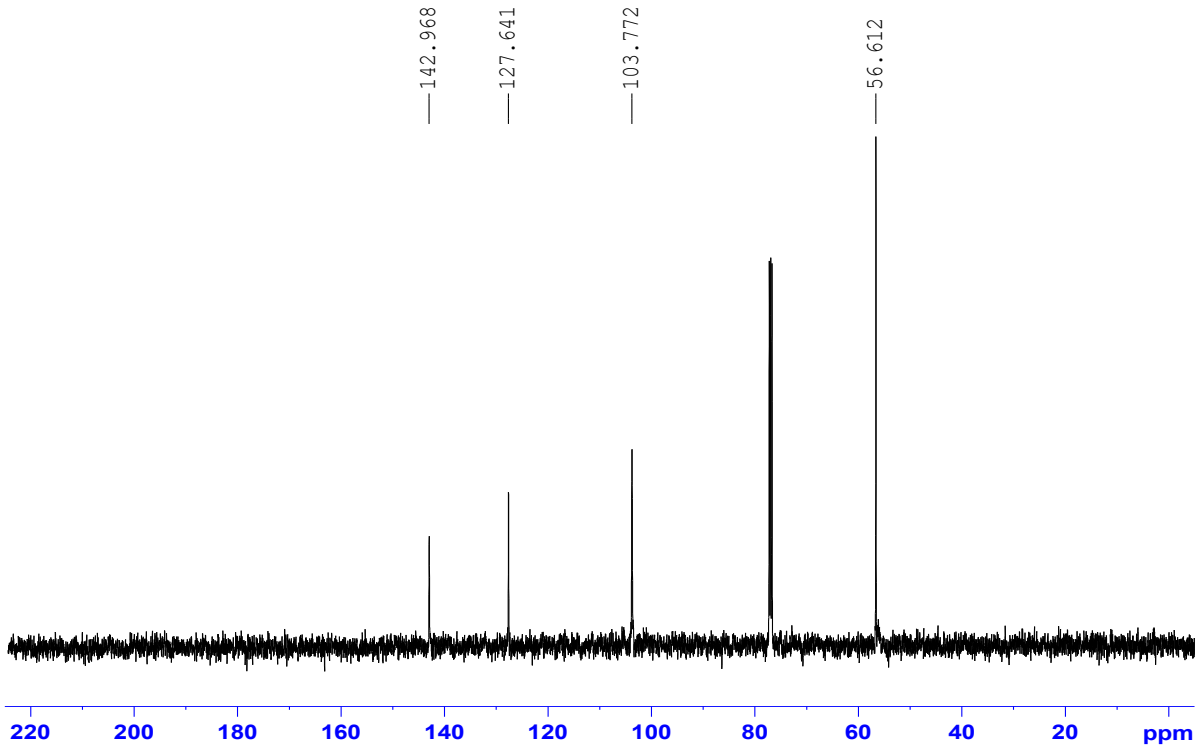

^{13}C NMR Spectrum of Compound 4 (Solvent: $CDCl_3$)

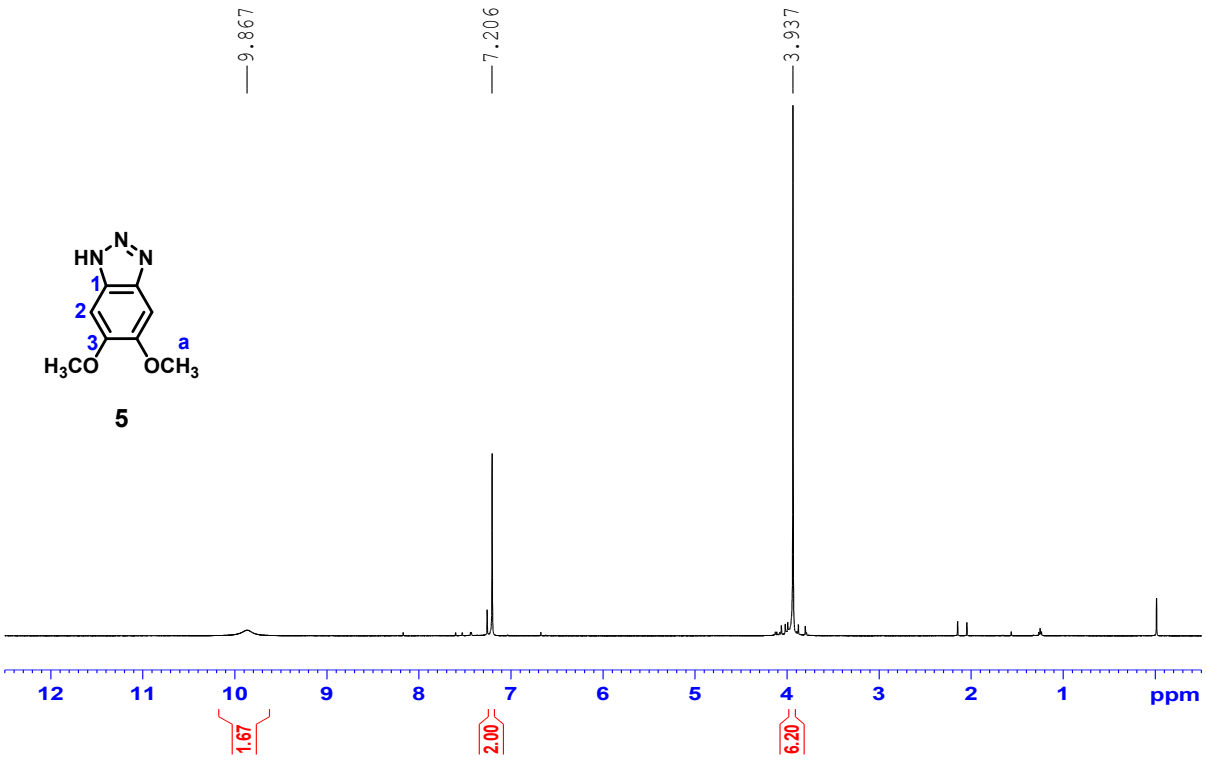

^{1}H NMR Spectrum of Compound 5 (Solvent: $CDCl_3$)

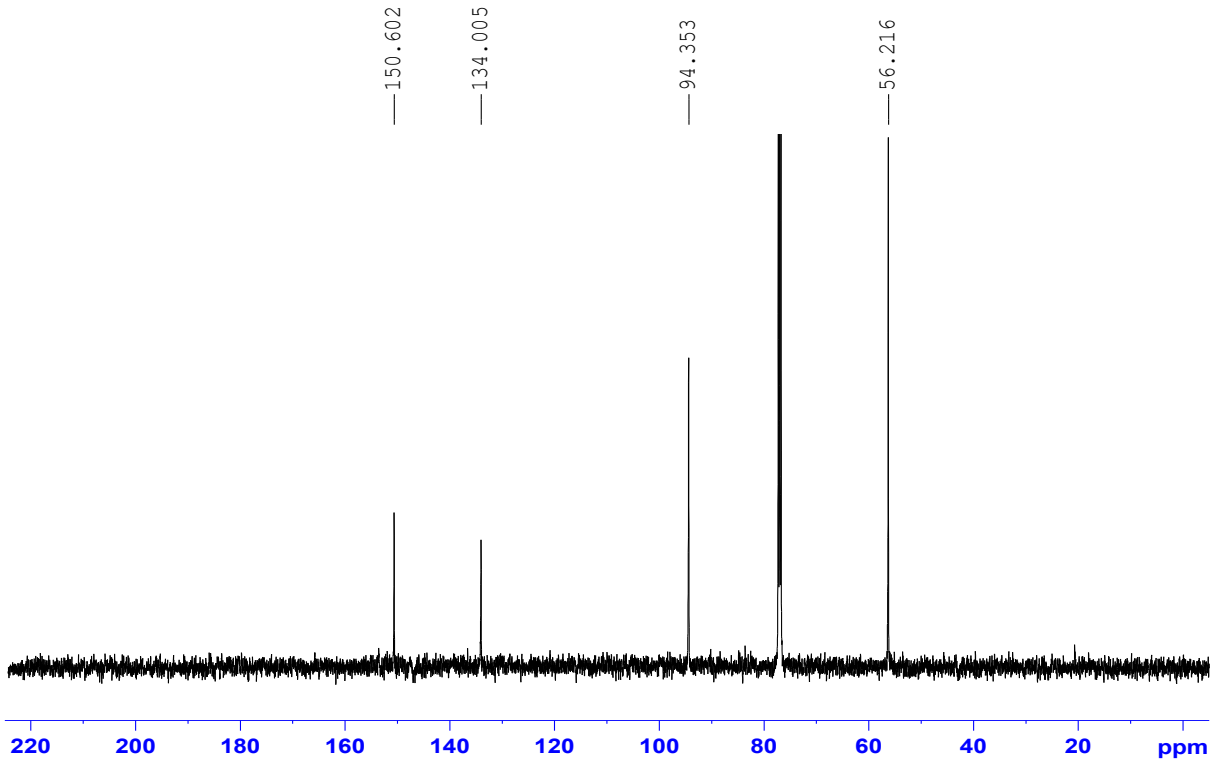

^{13}C NMR Spectrum of Compound 5 (Solvent: $CDCl_3$)

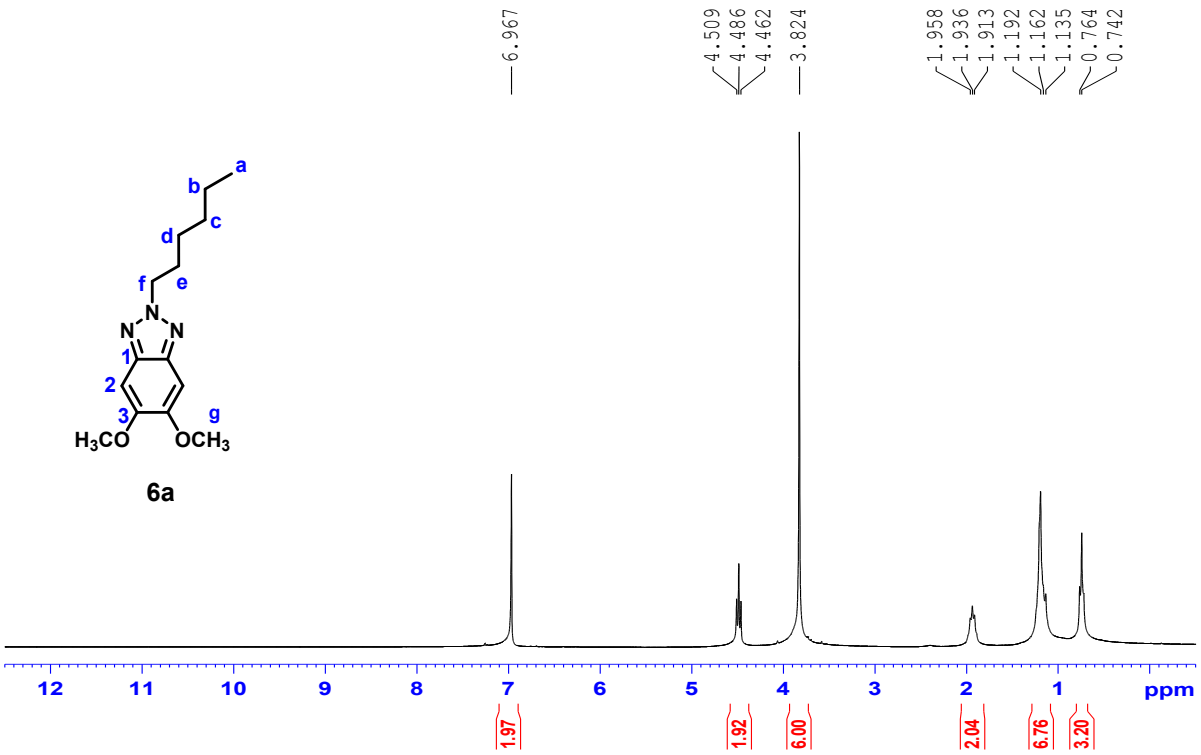

^{1}H NMR Spectrum of Compound 6a (Solvent: $CDCl_3$)

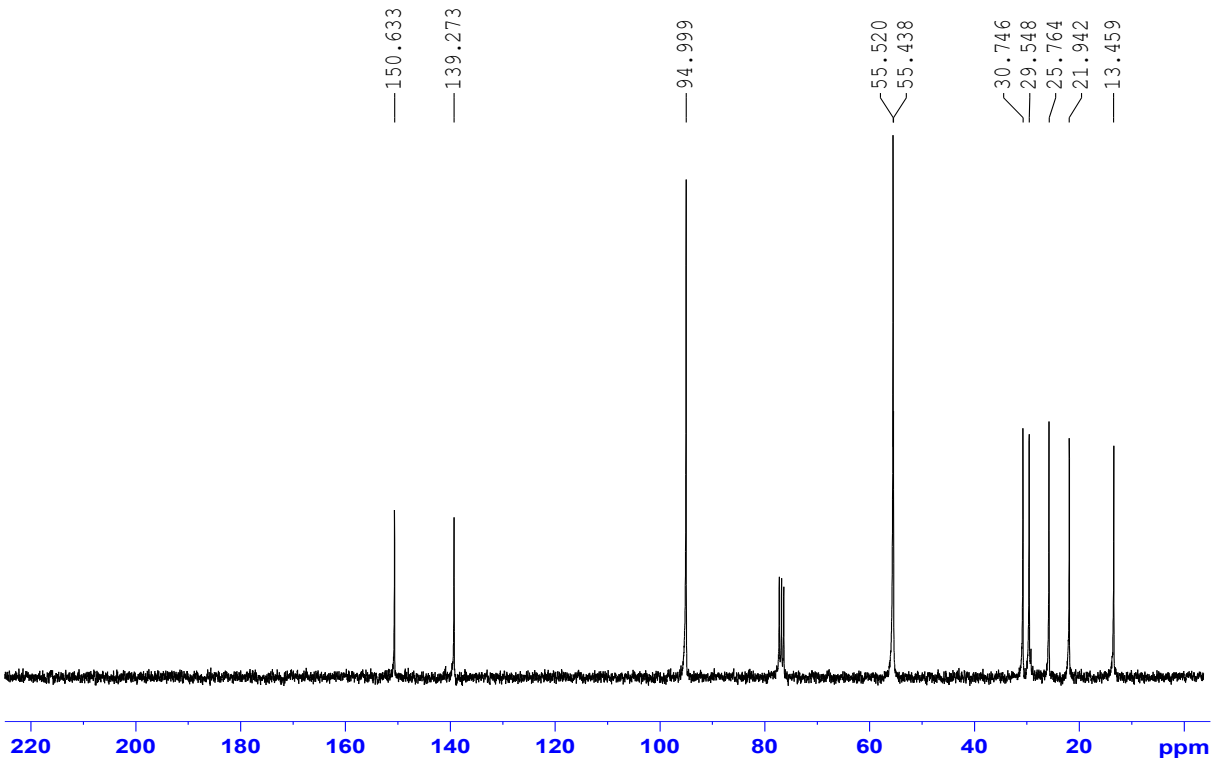

^{13}C NMR Spectrum of Compound 6a (Solvent: $CDCl_3$)

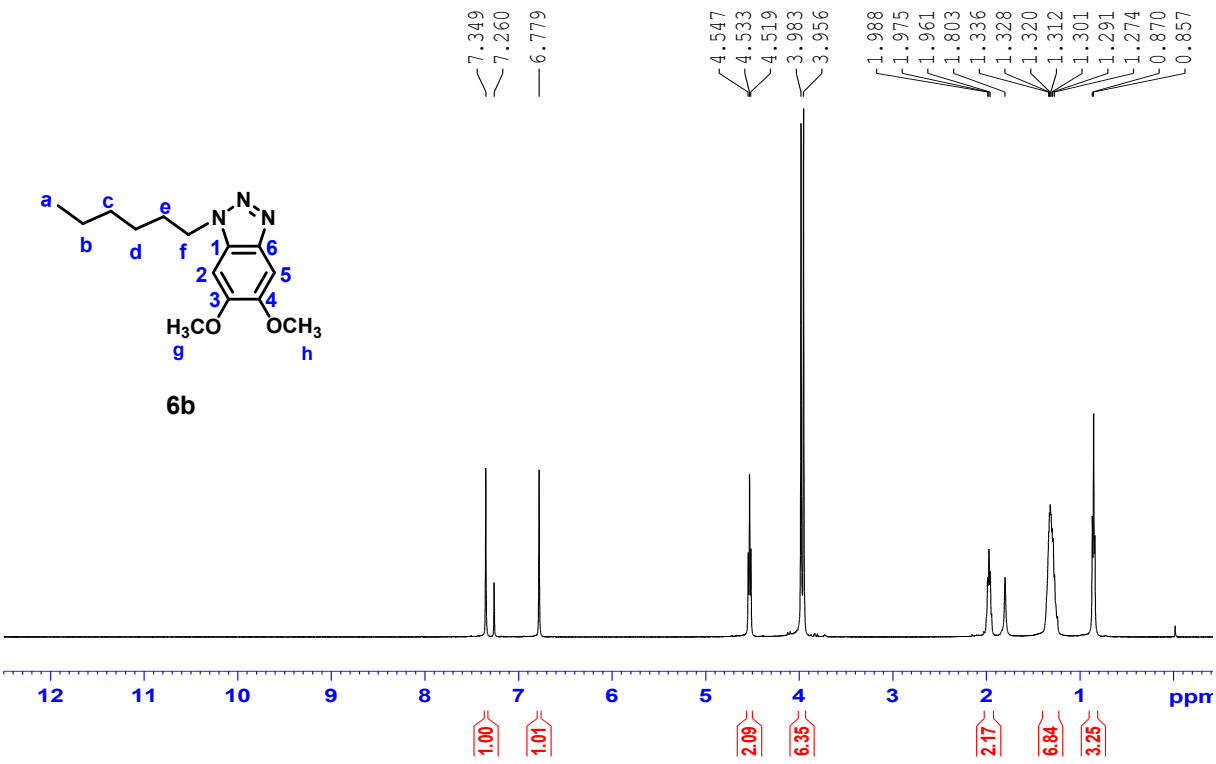

^{1}H NMR Spectrum of Compound 6b (Solvent: $CDCl_3$)

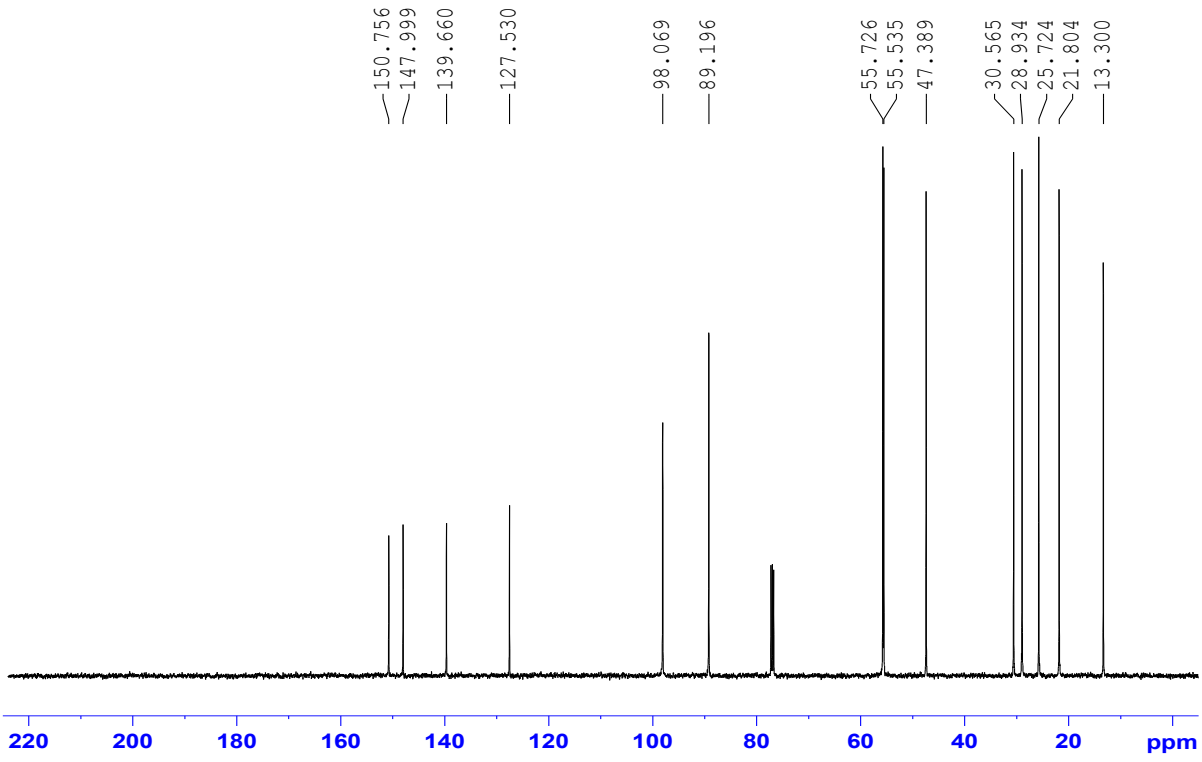

^{13}C NMR Spectrum of Compound 6b (Solvent: $CDCl_3$)

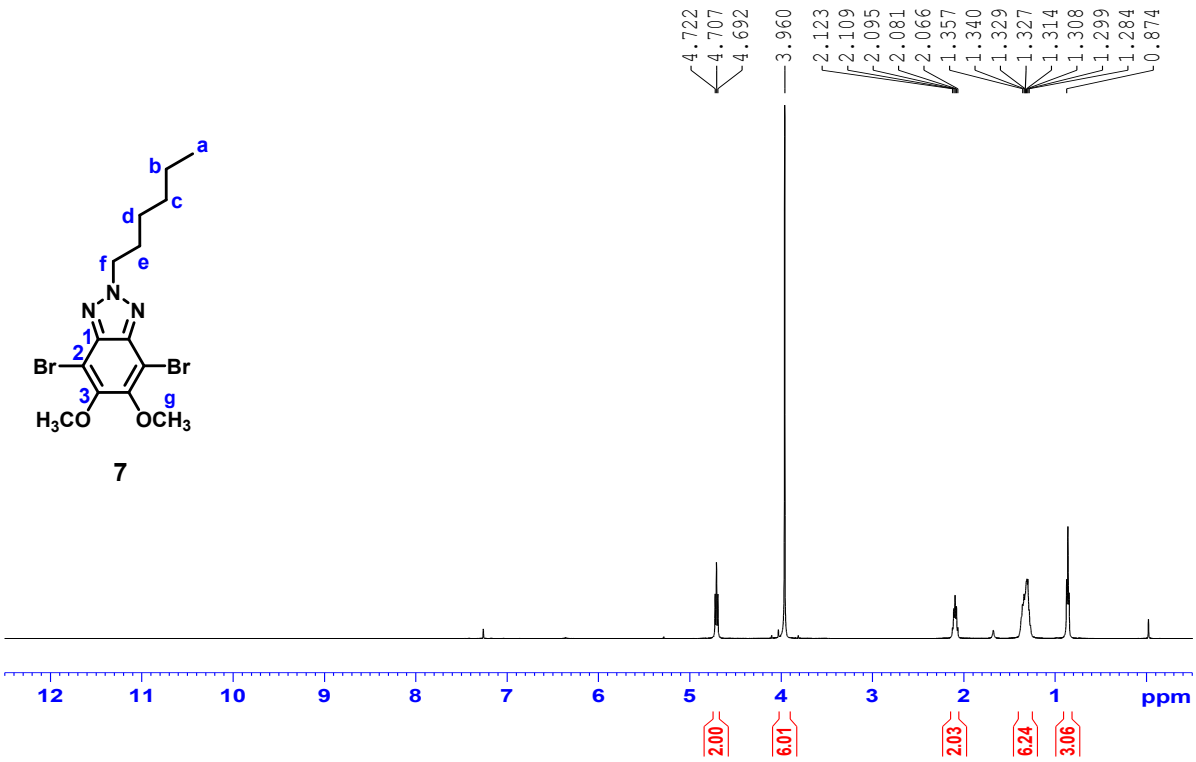

7

^{1}H NMR Spectrum of Compound 7 (Solvent: $CDCl_3$)

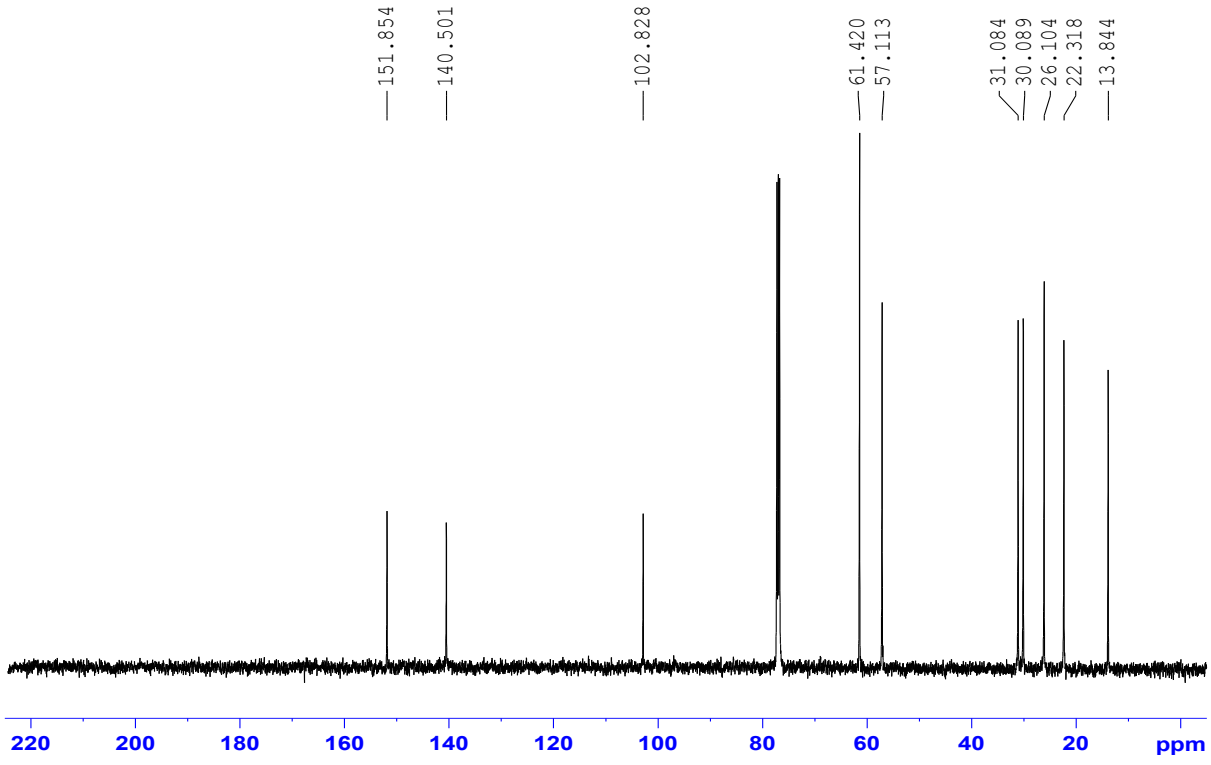

^{13}C NMR Spectrum of Compound 7 (Solvent: $CDCl_3$)

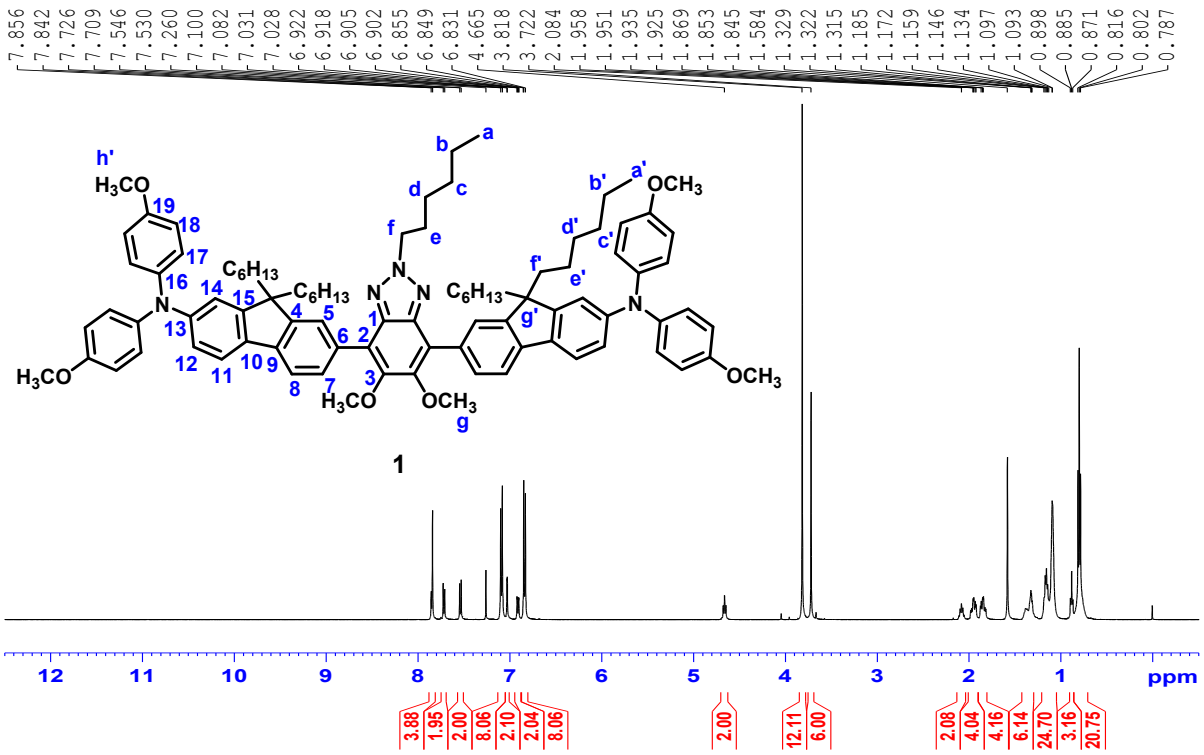

^{1}H NMR Spectrum of Compound 1 (Solvent: $CDCl_3$)

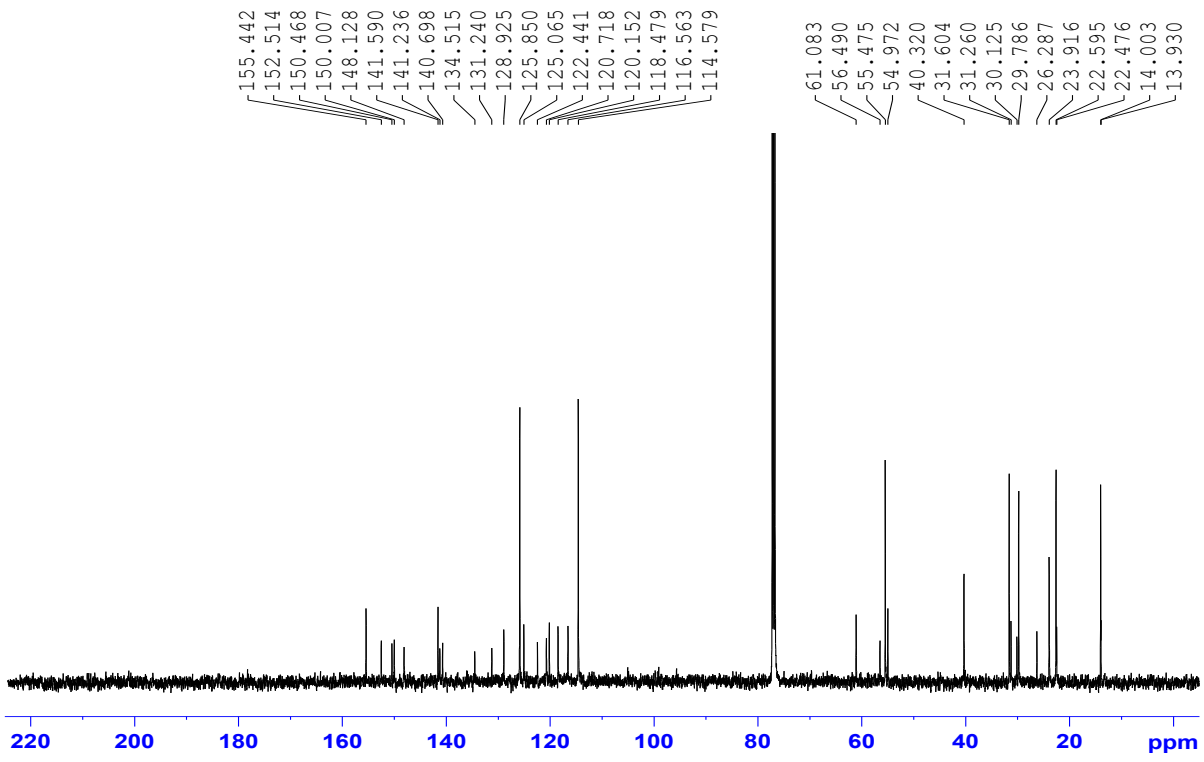

^{13}C NMR Spectrum of Compound 1 (Solvent: $CDCl_3$)

PL mapping of DC-SF film

To explore the uniformity of DC-SF neat film, we studied the PL mapping under the excitation of fs He-Cd CW laser with central wavelength at 325 nm. The pseudo maps of Figure S1 (a), (b), and (c) reveal the distribution of peak intensity, wavelength and the FWHM of DC-SF film with the size 500 μm × 500 μm. The corresponding distributions are shown by the histogram in Figs. S1 (d), (e), and (f).

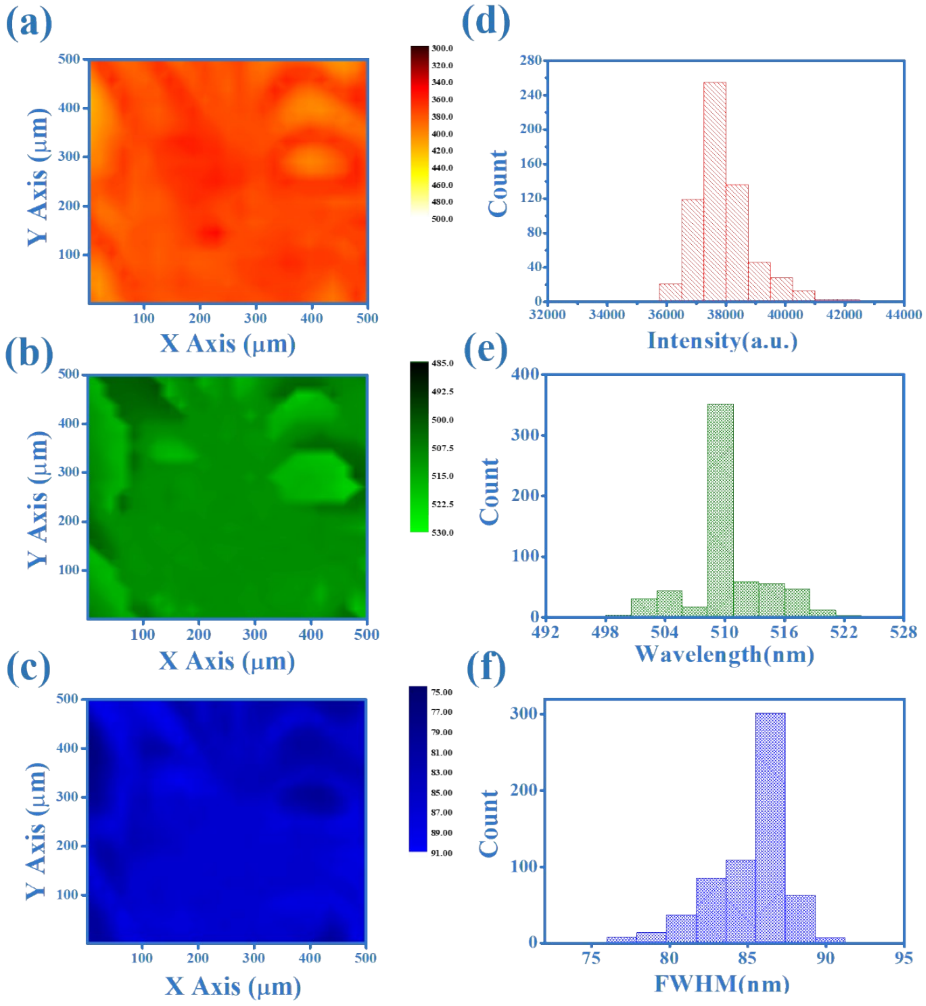

Figure S1. PL mapping image of (a) intensity, (b) wavelength and (c) FWHM on the DC-SF film, and the corresponding histograms of the (d) intensity, (e) wavelength and (f) FWHM distribution.

Lasing of D-A-D dye in solution phase state

We investigated the lasing behavior of organic D-A-D dye solution (~10^{-3} M) inside the polished quartz cuvette (with the dimension 12.5 mm × 7.5 mm) through the pump of Q-switched pulse. A cylindrical lens with focal length of about 75 mm was used to focused the pump stripe inside the cuvette. The image in Figure S2(a) depicts the dye solution under optical excitation. Once the pump fluence surpasses the lasing threshold, two distinct lasing spots are visibly projected onto the screen from both sides of the cuvette, as illustrated in Fig. S2(a). As depicted in Fig. S2(b), the evolution of the emission spectrum with increasing pump fluence reveals the appearance of multiple emission peaks. The Fabry-Perot lasing may be attributed to the multicavity structure formed by the two windows of the cuvette [1]. The wavelength of the highest emission peak, approximately 480.3 nm, is shorter than the peak wavelength of the photoluminescence (PL) emission, around 507 nm. The corresponding peak intensity (blue circle) and FWHM (red square) of the highest emission peak as a function of pump fluence are shown in Fig. S2(c). Based on the intersection of two linear fits of the peak intensity data, the lasing threshold is determined to be approximately 378.1 μJ/cm². The full width at half maximum (FWHM) notably decreases near this threshold, reaching a minimum value of around 1.7 nm at the highest pump fluence of 461.2 μJ/cm².

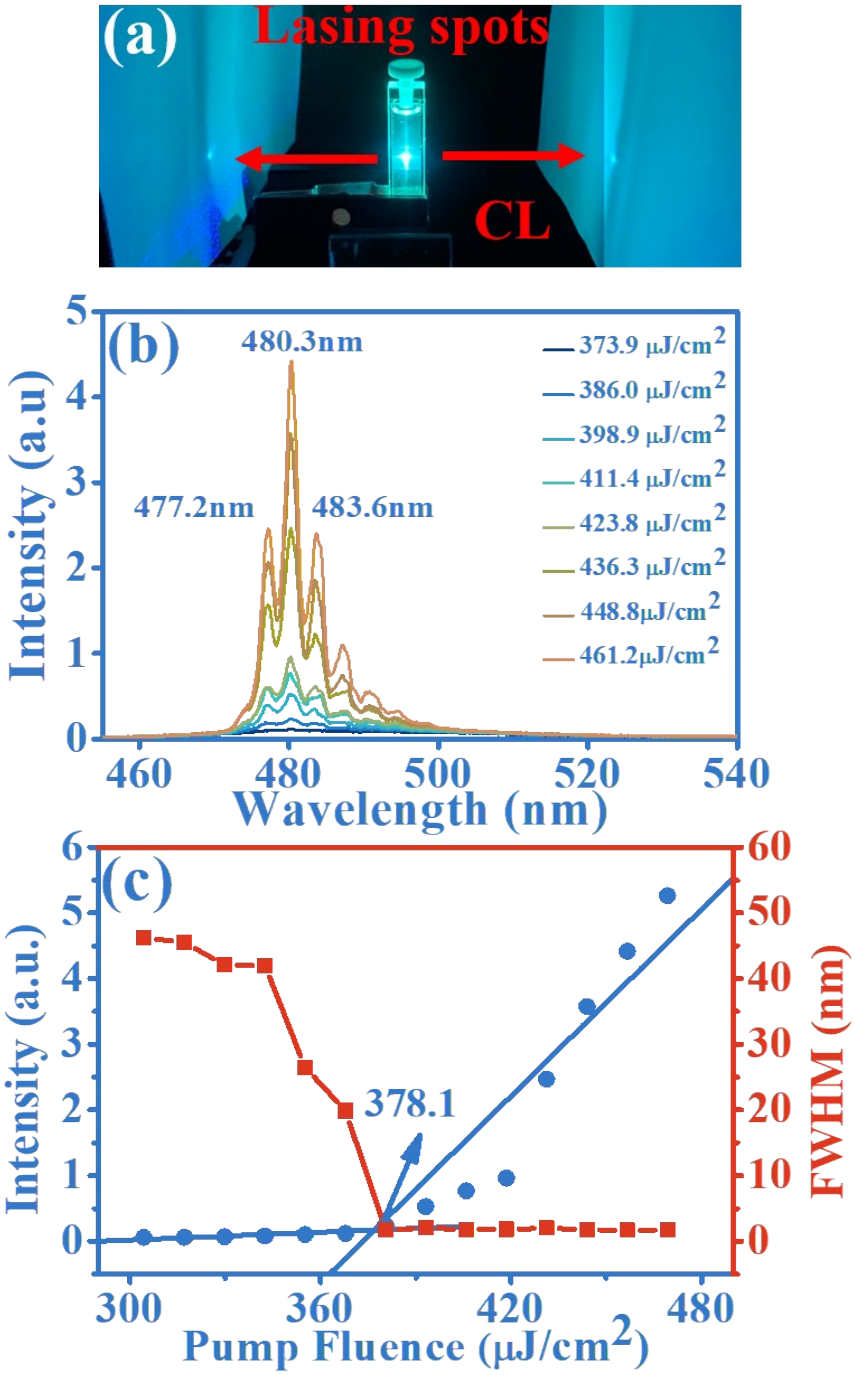

Figure S2. Lasing properties of 2OMe-DFL-OMeTr2 in the solution phase. (a) Photograph showing the lasing spots projected onto the screen from both sides of the dye solution in a cuvette, (b) evolution of the ASE spectra with increasing pump fluence, and (c) peak intensity (blue circles) and FWHM (red square) as functions of pump fluence.

Lasing of D-A-D dye in solid film state

In order to demonstrate the lasing behavior of synthesized D-A-D dye in solid state, the dye solution (with 10^{-3} M 2OMe-DFL-OmeTr2) was drop coated on top of biocompatible SF film. Besides, a flexible polyethylene terephthalate (PET) was adopted as a substrate. By means of the optical pulse excitation, the lasing spectrum from side of neat film was measured through spectrum meter. Figures S3 (a) and (b) show the evolution of emission spectrum from DC-SF film as pump fluence increases without (C=0 cm^{-1}) and with mechanical stress (C=0.45 cm^{-1}). Here, $C=1/R$ is the curvature of sample and R is radius of curvature. The corresponding photos of sample under pulse excitation are shown in the inset of these figures. Owing to the band filling effect, the ASE peak reveals slightly blue shift as pump fluence increases in both cases. Compared to Fig. S3(a), the peak intensity of the DC-SF film under bending conditions in Fig. S3(b) increases more rapidly with pump fluence, and the highest emission peak exhibits a slight red shift from 497.6 nm to 498.6 nm. The corresponding ASE peak intensity (blue circles) and FWHM (red square) as functions of pump fluence are presented in Figs. S3(b) and (c). The data indicate that the DC-SF neat film exhibits a lower lasing threshold, around 30.3 $\mu J/cm^2$, and higher slope efficiency under bending conditions. It is attributed to the slight enhancement of refractive index under bending condition to produce stronger light confinement.

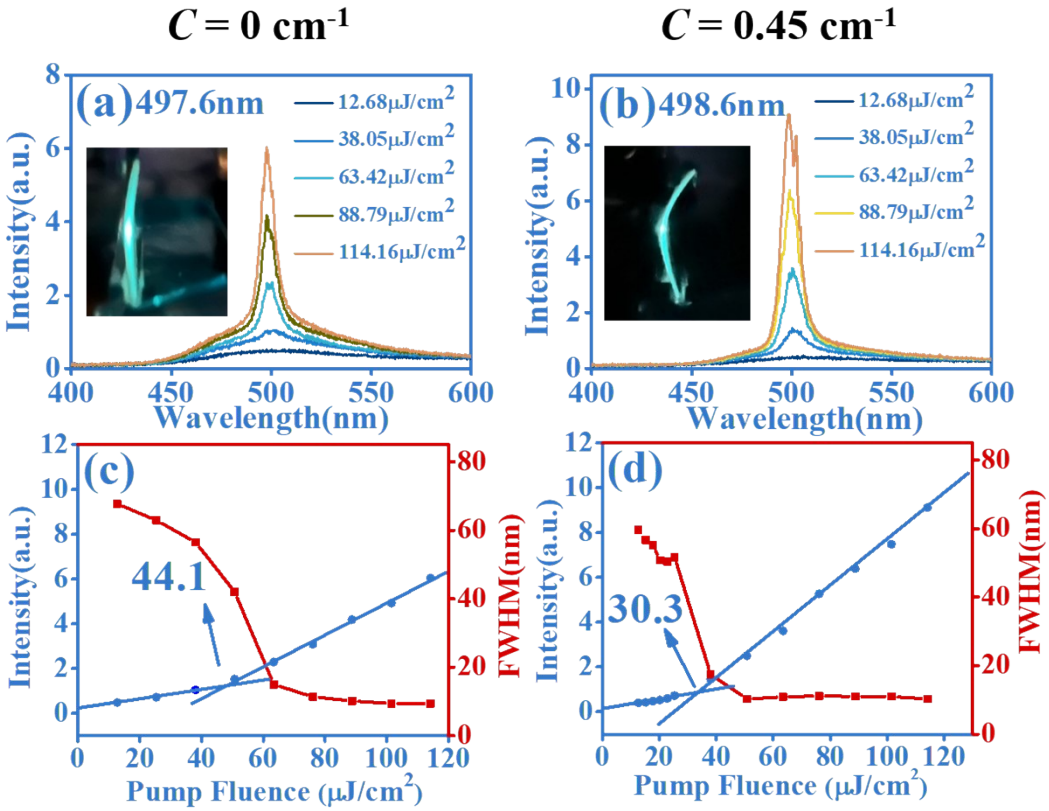

Figure S3. ASE of DC-SF neat film on flexible PET substrate. Evolution of ASE emission spectra as pump fluence increase for the neat film (a) without bending (C=0 cm^{-1}), (b) and under mechanical stress (C=0.45 cm^{-1}). The peak intensity (blue circle) and FWHM (red square) as function of pump fluence (c) without bending (C=0 cm^{-1}), (d) and under mechanical stress (C=0.45 cm^{-1}).

TPA-Induced PL at different excited wavelength

We studied the nonlinear absorption behavior of an organic D-A-D dye solution ($\sim 10^{-3}$ M) in a polished quartz cuvette (12.5 mm × 7.5 mm) by a passively mode-locked (PML) Ti:sapphire laser. Figure S4(a) shows the two-photon absorption photoluminescence (TPA-PL) spectra obtained under different excitation wavelengths of the PML Ti:sapphire laser. The TPA-PL spectrum is centered at 500.84 nm and exhibits a noticeable spectral shape shift toward longer wavelengths as the excitation wavelength increases. We also found that the fluorescence intensity reaches its maximum when the excitation wavelength is 750 nm. Fig. S4(b) summarizes the normalized PL intensity as a function of excitation wavelength, showing a clear resonance-like dependence that peaks at 750 nm and gradually decreases at longer wavelengths. This trend indicates a strong TPA process within this excitation range, where the efficiency of nonlinear absorption is maximized around 750 nm. The observed spectral shift and intensity variation reflect the interplay between the molecular electronic transition and the excitation photon energy, confirming the wavelength-dependent nature of the TPA-induced emission in the D-A-D dye solution.

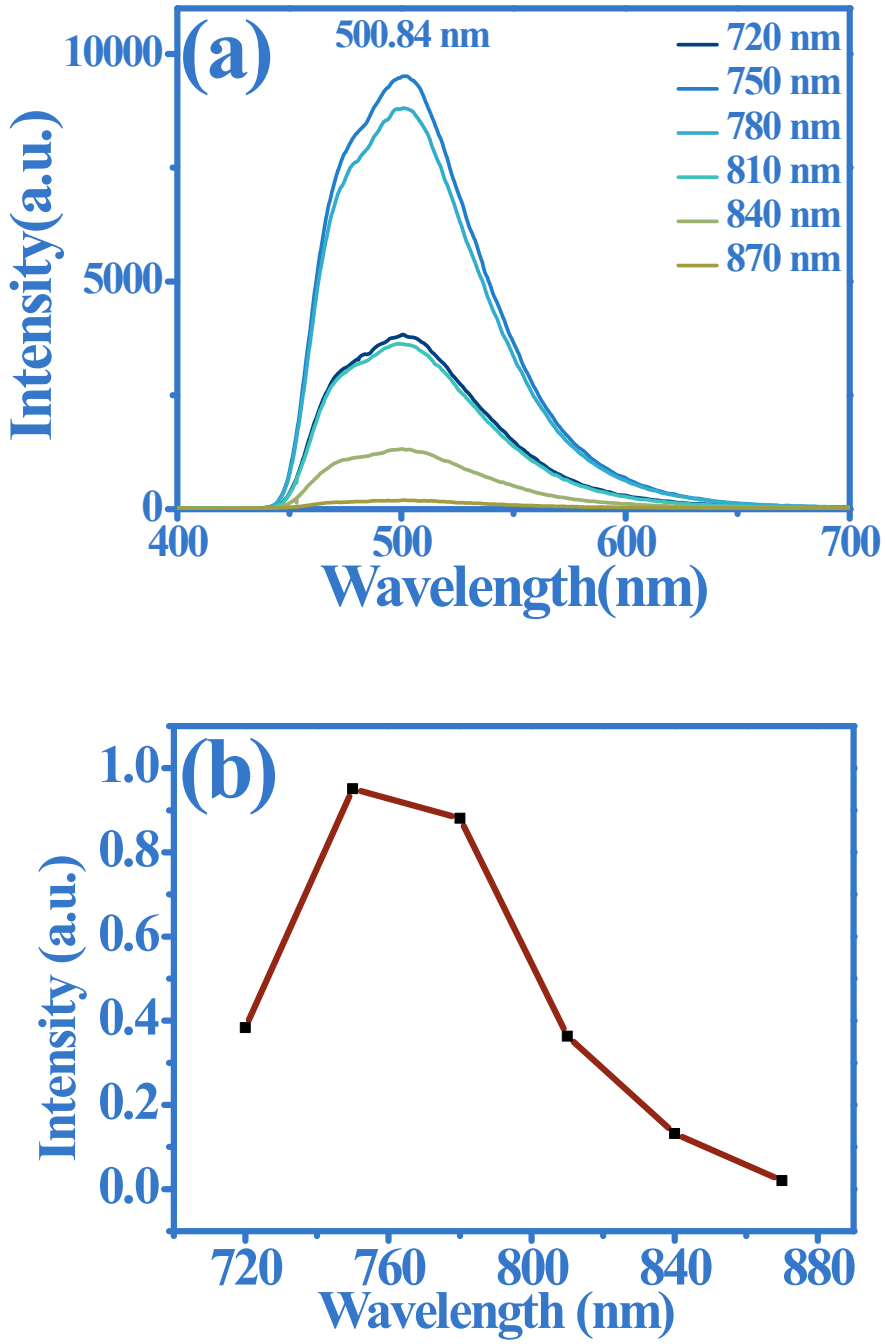

Figure S4. TPA characteristics of the D-A-D dye solution under different excitation wavelengths (720-870 nm) of the PML Ti:sapphire laser: (a) evolution of the TPA-induced PL spectra, and (b) the corresponding TPA-induced PL intensity as a function of excitation wavelength.

Gain coefficient from VSL method

The optical gain coefficient of active medium is the critical parameter to determine the threshold and slope efficiency of laser. Due to its simplicity of operation, the variable stripe length (VSL) method [2, 3] was adopted to obtain the optical gain coefficient of various active medium. As illustrated in the inset of Figure S5 (a), the pump beam was focused into a stripe-shape onto the DC-SF grating replica by a cylindrical lens. Through a movable blade, we varied the pump stripe length (L) to obtain the ASE spectrum from the side of the sample. In order to minimize diffraction effects, the slit is positioned close to the sample. Fig. S5 (a) shows the stripe-length-dependent emission spectra of sample under a pump fluence of 56.6 μJ/cm^2. Here, the single mode emission peak of DFB laser appears at 499.02 nm. The plot of lasing peak intensity variation as alternation of stripe length is shown in Fig. S5 (b). As population inversion is achieved at high pump fluence, an intense, narrower DFB lasing signal grows up exponentially with the excitation length (***L***), which can be described by [4]

$$I(L) = \left(\frac{A}{g}\right)(exp(gL) - 1)$$

Here ***I(L)*** is the emission intensity, ***g*** is the gain efficiency, ***L*** is the stripe length and ***A*** is the cross-sectional area of the excited volume, respectively. By the fitting (red lines), the optical gain coefficients of DC-SF grating replica in Fig. S5 (b) is 88.16 cm^{-1}.

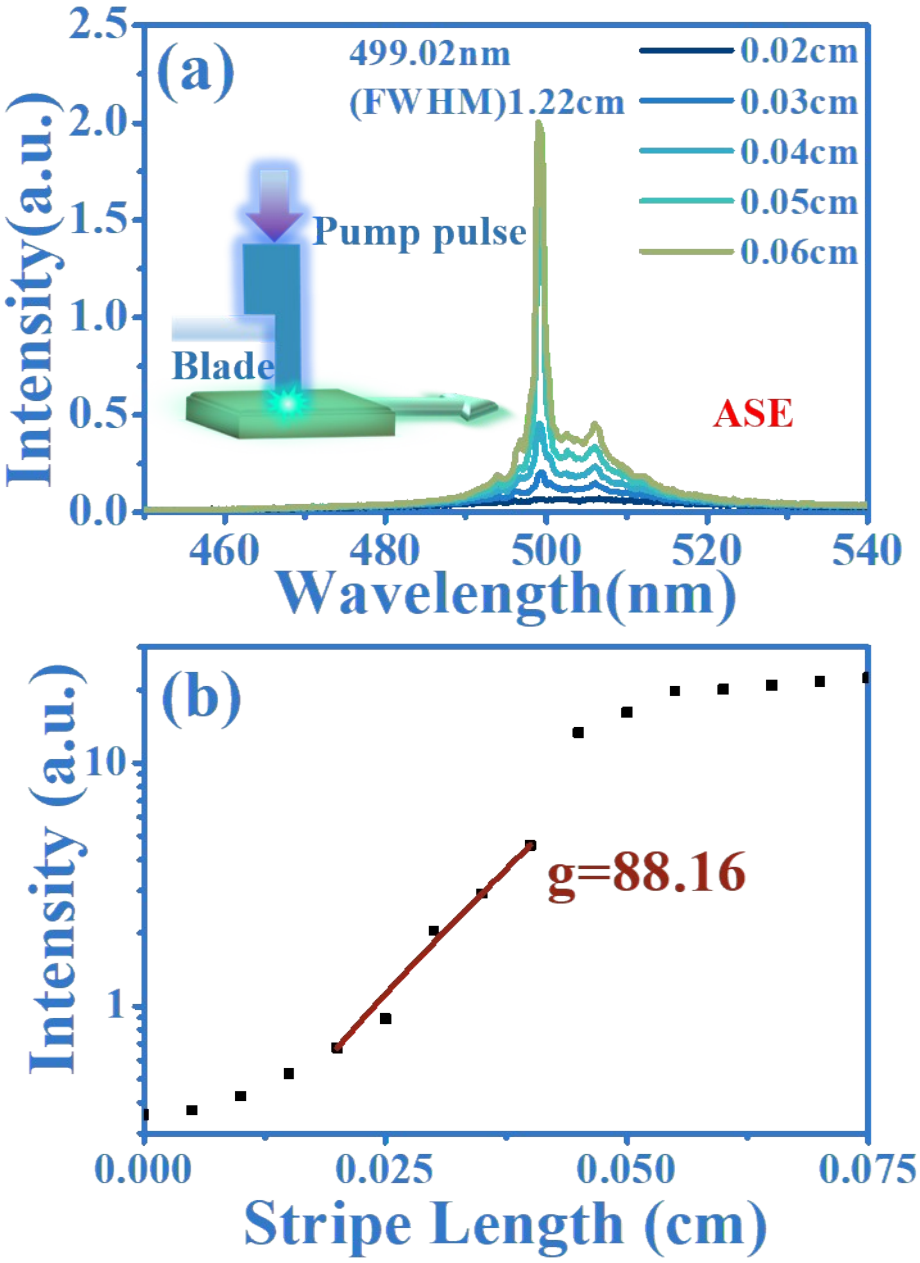

Figure S5. Gain coefficient measurement of DC-SF grating replica by VSL method (a) Emission spectrum of DC-SF replica grating (inset is schematic setup of VSL method by Q-Switch laser) (b) Gain coefficient measurement of DC-SF grating replica.

References

1. G. S. He, R. Signorini, and P. N. Prasad, "Two-photon-pumped frequency-upconverted blue lasing in Coumarin dye solution," Applied optics **37**, 5720-5726 (1998).
2. L. D. Negro, P. Bettotti, M. Cazzanelli, D. Pacifici, and L. Pavesi, "Applicability conditions and experimental analysis of the variable stripe length method for gain measurements," Optics Communications **229**, 337-348 (2004).
3. A. L. Alvarado-Leaños, D. Cortecchia, G. Folpini, A. R. Srimath Kandada, and A. Petrozza, "Optical Gain of Lead Halide Perovskites Measured via the Variable Stripe Length Method: What We Can Learn and How to Avoid Pitfalls," Advanced Optical Materials **9** (2021).
4. K. Dridi, A. Benhsaien, J. Zhang, and T. J. Hall, "Narrow Linewidth 1550 nm Corrugated Ridge Waveguide DFB Lasers," IEEE Photonics Technology Letters **26**, 1192-1195 (2014).